Nuclear Inst. and Methods in Physics Research, A 867 (2017) 15–19

Contents lists available at ScienceDirect

Nuclear Inst. and Methods in Physics Research, A

journal homepage: www.elsevier.com/locate/nima

A fast numerical integrator for relativistic charged particle tracking

Ji Qiang

Lawrence Berkeley National Laboratory, Berkeley, CA 94720, USA

ARTICLE INFO

Keywords:
Numerical integrator
Relativistic charged particle

ABSTRACT

In this paper, we report on a fast second-order numerical integrator to solve the Lorentz force equations of a relativistic charged particle in electromagnetic fields. This numerical integrator shows less numerical error than the popular Boris algorithm in tracking the relativistic particle subject to electric and magnetic space-charge fields and requires less number of operations than another recently proposed relativistic integrator.

1. Introduction

Numerical tracking charged particle motion in electric and magnetic fields has many applications in beam physics and plasma physics. This normally involves solving the Lorentz force equations with electromagnetic fields numerically. A popular method to solve the Lorentz equation subject to electromagnetic fields is the Boris integrator [1]. This integrator is time reversible and preserves phase space volume [2,3]. These properties make it suitable for long-term particle tracking. However, in recent study of the relativistic electron beam dynamics subject to its space-charge fields, we observed large numerical errors using the Boris integrator. These errors result from updating momenta using electric field and magnetic field in separate steps. For the space-charge forces in laboratory frame, there is a large cancellation between the electric field contribution and the magnetic field contribution in the Lorentz force equation, which results in $1/\gamma^2$ decrease of the transverse space charge forces in the laboratory frame. Here, $\gamma = E/mc^2 + 1$ is the relativistic factor, E the kinetic energy of the particle, m the rest mass of the particle, and the c the speed of light in vacuum. The lack of appropriate cancellation of electric and magnetic forces in the Boris integrator for a relativistic charged particle causes significant error in numerical tracking. The problem of using the Boris algorithm for relativistic charged particle was also observed in another early study [4]. By taking infinite limit of the relativistic factor, the author of reference [4] observed that the Boris algorithm would bear no physical solutions. A new time-reversible second-order numerical integrator was proposed in reference [4] for relativistic charged particle tracking. This integrator works properly with large relativistic factor but is more mathematically complex and also requires more numerical operations than the Boris integrator.

In this paper, we propose a new fast second-order integrator that works well with large relativistic factor and also requires less numerical operations than the Boris integrator for relativistic charged particle tracking. The organization of this paper is as follows: after the introduction, we present the fast second-order numerical integrator in Section 2; We present numerical tests of the integrator in Section 3 and draw conclusions in Section 4.

2. Fast second-order numerical integrator

The Lorentz equations of motion for a charged particle subject to electric and magnetic fields can be written as:

$$\frac{d\mathbf{r}}{dt} = \frac{\mathbf{p}c}{\gamma} \tag{1}$$

$$\frac{d\mathbf{p}}{dt} = q\left(\frac{\mathbf{E}}{mc} + \frac{1}{m\gamma}\mathbf{p}\times\mathbf{B}\right) \tag{2}$$

where $\mathbf{r} = (x, y, z)$ denotes the particle spatial coordinates, $\mathbf{p} = (p_x/mc, p_y/mc, p_z/mc)$ the particle normalized mechanic momentum, m the particle rest mass, q the particle charge, c the speed of light in vacuum, γ the relativistic factor defined by $\sqrt{1+\mathbf{p}\cdot\mathbf{p}}$, t the time, $\mathbf{E}(x, y, z, t)$ the electric field, and $\mathbf{B}(x, y, z, t)$ the magnetic field. Instead of using the time t as an explicit independent variable, we rewrite the above equations using s as independent variable:

$$\frac{dt}{ds} = 1 \tag{3}$$

$$\frac{d\mathbf{r}}{ds} = \frac{\mathbf{p}c}{\gamma} \tag{4}$$

E-mail address: jqiang@lbl.gov.

http://dx.doi.org/10.1016/j.nima.2017.04.015
Received 13 March 2017; Accepted 10 April 2017
Available online 12 April 2017
0168-9002/

$$\frac{d\mathbf{p}}{ds} = q\left(\frac{\mathbf{E}}{mc} + \frac{1}{m\gamma}\mathbf{p}\times\mathbf{B}\right) \quad (5)$$

Letting $\zeta(t, \mathbf{r}, \mathbf{p} : s)$ denote a vector of coordinates, the above equations of motion can be rewritten as:

$$\frac{d\zeta}{ds} = A\zeta \quad (6)$$

where the matrix A is a given as:

$$A = \begin{pmatrix} 1/t & 0 & 0 \\ 0 & 0 & c/\gamma \\ 0 & q\mathbf{E}/(mc\mathbf{r}) & q\mathbf{1}\times\mathbf{B}/(m\gamma) \end{pmatrix} \quad (7)$$

A formal solution for above equation after a single step τ can be written as:

$$\zeta(\tau) = \exp(A\tau)\zeta(0) \quad (8)$$

The matrix A can be written as a sum of two terms $A = B + C$, where

$$B = \begin{pmatrix} 1/t & 0 & 0 \\ 0 & 0 & c/\gamma \\ 0 & 0 & 0 \end{pmatrix} \quad (9)$$

and

$$C = \begin{pmatrix} 0 & 0 & 0 \\ 0 & 0 & 0 \\ 0 & q\mathbf{E}/(mc\mathbf{r}) & q\mathbf{1}\times\mathbf{B}/(m\gamma) \end{pmatrix} \quad (10)$$

Using the Baker-Campbell-Hausdorff theorem [5–7], a second-order approximation for above single step solution can be obtained as:

$$\begin{aligned} \zeta(\tau) &= \exp(\tau(B+C))\zeta(0) \\ &= \exp(\frac{1}{2}\tau B)\exp(\tau C)\exp(\frac{1}{2}\tau B)\zeta(0) + O(\tau^3) \end{aligned} \quad (11)$$

Letting $\exp(\frac{1}{2}\tau B)$ define a transfer map $\mathcal{M}_1$ and $\exp(\tau C)$ a transfer map $\mathcal{M}_2$, for a single step, the above splitting results in a second-order numerical integrator for the original equation as:

$$\begin{aligned} \zeta(\tau) &= \mathcal{M}(\tau)\zeta(0) \\ &= \mathcal{M}_1(\tau/2)\mathcal{M}_2(\tau)\mathcal{M}_1(\tau/2)\zeta(0) + O(\tau^3) \end{aligned} \quad (12)$$

From definitions of the matrices B and C, it is seen that the transfer map $\mathcal{M}_1$ corresponds to the solutions of Eqs. (3) and (4) for half step, and the transfer map $\mathcal{M}_2$ corresponds to the solution of Eq. (5) for one step. The solution of the transfer map $\mathcal{M}_1(\tau/2)$ is straightforward and can be written as:

$$t(\tau/2) = t(0) + \frac{\tau}{2} \quad (13)$$

$$\mathbf{r}(\tau/2) = \mathbf{r}(0) + \frac{\tau\mathbf{p}}{2\gamma} \quad (14)$$

The $\mathcal{M}_2(\tau)$ can have different second-order solutions depending on different ways of approximation. In the Boris algorithm, $\mathcal{M}_2(\tau)$ is given as:

$$\mathbf{p}_- = \mathbf{p}(0) + \frac{q\mathbf{E}\tau}{2mc} \quad (15)$$

$$\gamma_- = \sqrt{1 + \mathbf{p}_-\cdot\mathbf{p}_-} \quad (16)$$

$$\mathbf{p}_+ - \mathbf{p}_- = (\mathbf{p}_+ + \mathbf{p}_-)\times\frac{q\mathbf{B}\tau}{2\,m\gamma_-} \quad (17)$$

$$\mathbf{p}(\tau) = \mathbf{p}_+ + \frac{q\mathbf{E}\tau}{2mc} \quad (18)$$

where $\mathbf{p}_+$ can be solved analytically from the linear equation Eq. (17). The Boris algorithm is time-reversible and has been widely used in numerical plasma and beam physics simulations [8–11]. The particle momenta are updated using electric force in Eqs. (15) and (18), and using magnetic force in Eq. (17). The lack of direct cancellation from electric fields and magnetic fields can introduce large error to simulate relativistic charged particles including space-charge effects, where the electric field and the magnetic field cancel each other significantly in the laboratory frame and results in $1/\gamma^2$ decrease of the transverse space-charge forces.

The time-reversible solution for $\mathcal{M}_2(\tau)$ proposed in reference [4] is given as:

$$\gamma_0 = \sqrt{1 + \mathbf{p}\cdot\mathbf{p}} \quad (19)$$

$$\mathbf{p}_- = \mathbf{p}(0) + \frac{q\tau}{2mc}(\mathbf{E} + c\mathbf{p}/\gamma_0\times\mathbf{B}) \quad (20)$$

$$\mathbf{p}_+ = \mathbf{p}_- + \frac{q\mathbf{E}\tau}{2mc} \quad (21)$$

$$\gamma_1 = \sqrt{1 + \mathbf{p}_+\cdot\mathbf{p}_+} \quad (22)$$

$$\mathbf{t} = \frac{q\mathbf{B}\tau}{2\,m} \quad (23)$$

$$\lambda = \mathbf{p}_+\cdot\mathbf{t} \quad (24)$$

$$\sigma = \gamma_1^2 - \mathbf{t}\cdot\mathbf{t} \quad (25)$$

$$\gamma_2 = \sqrt{\frac{\sigma + \sqrt{\sigma^2 + 4(\mathbf{t}\cdot\mathbf{t} + \lambda^2)}}{2}} \quad (26)$$

$$\mathbf{t}^* = \mathbf{t}/\gamma_2 \quad (27)$$

$$s = 1/(1 + \mathbf{t}^*\cdot\mathbf{t}^*) \quad (28)$$

$$\mathbf{p}(\tau) = s[\mathbf{p}_+ + (\mathbf{p}_+\cdot\mathbf{t}^*)\mathbf{t}^* + \mathbf{p}_+\times\mathbf{t}^*] \quad (29)$$

This algorithm works well for charged particle tracking with large relativistic factor. However, it is also mathematically more complex than the Boris algorithm and requires more numerical calculation than the Boris integrator does.

The source of error in the Boris algorithm results from the lacking appropriate cancellation of the electric force and the magnetic force in the space-charge fields. This can be solved by updating the momenta using both electric force and magnetic force in the same step instead of separate steps. Here, we propose a new second-order integrator for transfer map $\mathcal{M}_2(\tau)$ as follows:

$$\mathbf{p}_- = \mathbf{p}(0) + \frac{q}{mc}(\mathbf{E} + \mathbf{v}(0)\times\mathbf{B})\tau \quad (30)$$

$$\mathbf{v}_+ = \frac{\mathbf{v}(0) + \mathbf{v}_-}{2} \quad (31)$$

$$\mathbf{p}(\tau) = \mathbf{p}(0) + \frac{q}{mc}(\mathbf{E} + \mathbf{v}_+\times\mathbf{B})\tau \quad (32)$$

where $\mathbf{v} = \mathbf{p}c/\gamma$. This algorithm includes the direct cancellation of the electric force and the magnetic force from the space-charge fields and works well for large relativistic factor. It has a simple mathematical form and also requires less numerical operations than the Boris integrator and the Vay integrator.

3. Numerical tests

We tested the above new second-order integrator using several numerical examples. In the first example, we considered an electron moving inside the static electric and magnetic fields generated by a co-moving positron beam. These fields are given as:

$$E_x = E_0 x \gamma_0 \tag{33}$$

$$E_y = E_0 y \gamma_0 \tag{34}$$

$$E_z = 0 \tag{35}$$

$$B_x = -E_0 y \gamma_0 \beta_0 / c \tag{36}$$

$$B_y = E_0 x \gamma_0 \beta_0 / c \tag{37}$$

$$B_z = 0 \tag{38}$$

where γ_0 is the relativistic factor of the moving positron beam, $\beta_0 = \sqrt{1-(1/\gamma_0)^2}$, and the constant $E_0 = 9\times 10^6\ V/m^2$. The above fields correspond to the space-space fields generated by the co-moving infinitely long transversely uniform cylindrical positron beam.

First, we assume that both the initial electron kinetic energy and the co-moving positron beam kinetic energy are 50 MeV. Fig. 1 shows the electron transverse trajectory (x) evolution as a function of time from the Boris integrator (magenta), the Vay integrator (green), the new integrator (blue) with a step size of 1 ns (around 0.002 oscillation period), and the approximate analytical solution (red). Here, the analytical solution is obtained in the co-moving frame without including the relativistic effects and then Lorentz transformed back to the laboratory frame. The analytical solution for the x trajectory starting with initial 0 momentum is given as:

$$x(t) = x_0 \cos(\sqrt{qE_0/m}/\gamma_0 t) \tag{39}$$

where $x_0 = 1$ mm is the initial horizontal position. We see that all solutions agree well with each other for the first couple of oscillation periods. The solution from the Boris integrator starts to deviate from the other solutions while the other three solutions are still on top of each other.

Fig. 2 shows the relative numerical errors at the end of the above integration as a function of step size from the Boris integrator (magenta), the Vay integrator (green), and the new proposed integrator (blue) together with a quadratic monomial function (red). It is seen that all three numerical integrators converge as 2^{nd} power with respect to the step size. However, the Boris integrator yields much larger errors than the Vay integrator and the new integrator in this example. The Vay integrator and the new integrator barely show any noticeable difference in this example.

Next, we assumed that both the initial electron and the co-moving positron beam have a kinetic energy of 100 MeV. Fig. 3 shows the electron x coordinate evolution as a function of time from the Boris integrator (magenta), the Vay integrator (green), the new integrator (blue) with a step size of 1 ns (around 0.001 oscillation period), and the analytical solution (red).

It is seen that even after one oscillation period, the solution from the Boris integrator starts to deviate from the other solutions while the other three solutions are still on top of each other. Fig. 4 shows the relative numerical errors at the end of the above integration as a function of time step size from the Boris integrator, the Vay integrator, and the new integrator.

As expected, all three second-order accuracy numerical integrators converge as power of 2 with respect to the time step size. However, the errors from the Boris integrator are about 4 orders of magnitude larger than those from the other two integrators. These errors become worse in this example (100 MeV) compared with those in the 50 MeV example.

In the second example, we tracked a 100 MeV electron in above electric and magnetic fields for more 500,000 periods using the new second-order numerical integrator with time step size of 100 ns. The relative kinetic energy growth as a function of time is shown in Fig. 5. It is seen that except the oscillation from energy exchange, there is no steady state secular energy increase or decrease resulting from numerical heating or damping of the proposed new integrator.

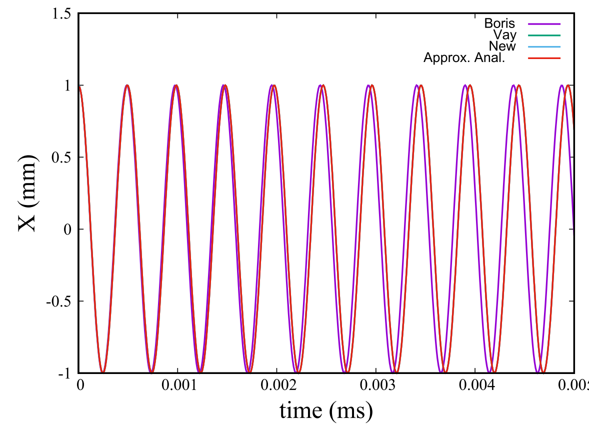

Fig. 1. Particle x coordinate evolution as a function of time from the Boris integrator (magenta), the Vay integrator (green), the new integrator (blue), and the analytical solution for an electron with 50 MeV kinetic energy (red). (For interpretation of the references to color in this figure legend, the reader is referred to the web version of this article.)

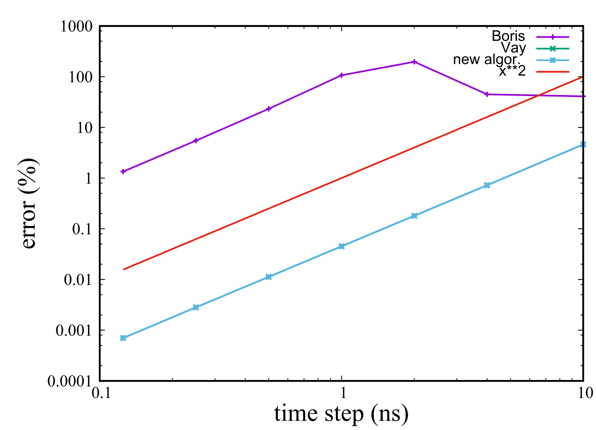

Fig. 2. Relative numerical errors at the end of the above integration as a function of step size from the Boris integrator (magenta), the Vay integrator (green), the new integrator (blue), and the analytical solution for an electron with 50 MeV kinetic energy. A quadratic monomial function is also plotted here (red). (For interpretation of the references to color in this figure legend, the reader is referred to the web version of this article.)

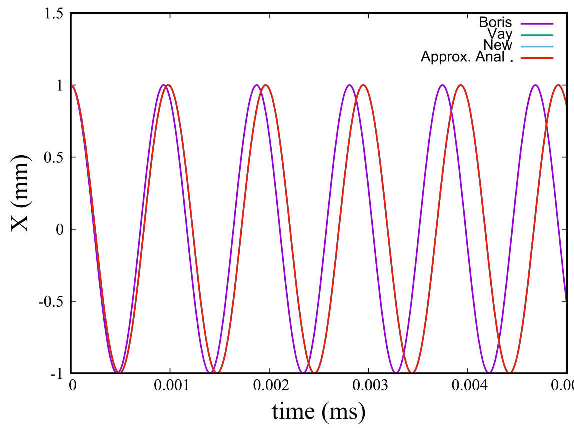

Fig. 3. Particle x coordinate evolution as a function of time from the Boris integrator (magenta), the Vay integrator (green), the new integrator (blue), and the analytical solution (red) for an electron with 100 MeV kinetic energy. (For interpretation of the references to color in this figure legend, the reader is referred to the web version of this article.)

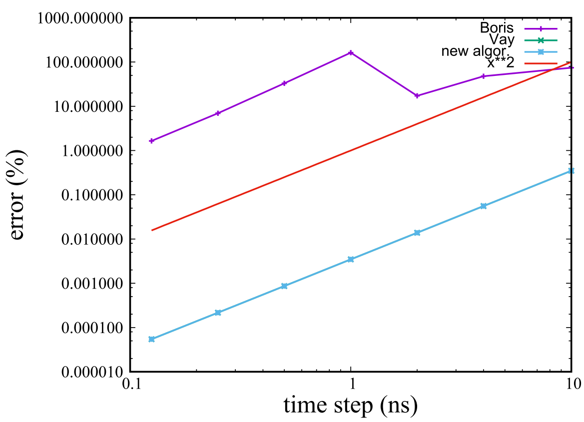

Fig. 4. Relative numerical errors at the end of the above integration as a function of step size from the Boris integrator (magenta), the Vay integrator (green), and the new integrator (blue) for an electron with 100 MeV kinetic energy. A quadratic monomial function is also plotted here (red). (For interpretation of the references to color in this figure legend, the reader is referred to the web version of this article.)

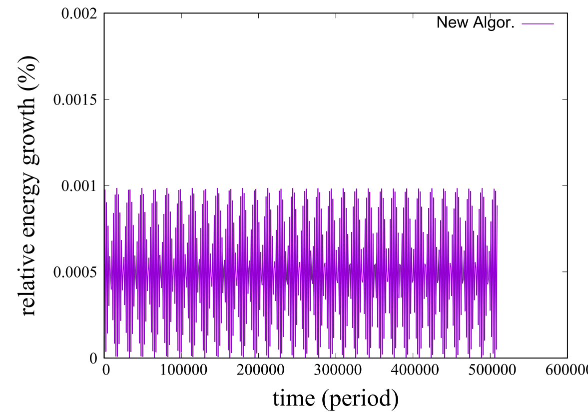

Fig. 5. Relative kinetic energy growth evolution of an initial 100 MeV electron.

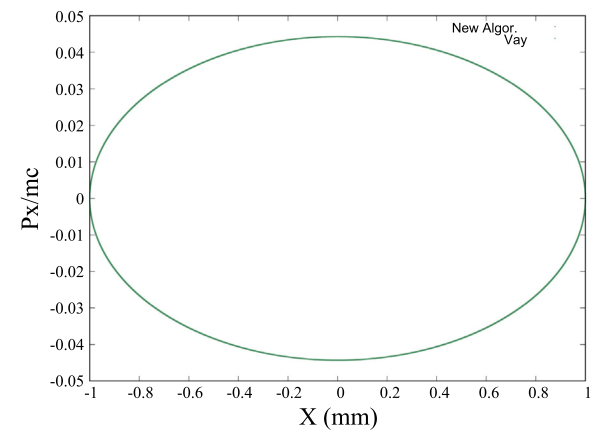

Fig. 6. Electron phase space trajectory from the new integrator and the Vay integrator.

Fig. 6 shows the phase space trajectory of the electron from the proposed new algorithm and from the Vay algorithm. It is seen that both integrators agree with each other very well. The phase space structure is well preserved after 500,000 periods.

In the third numerical example, we simulated a 1 nC electron beam with an initial 50 MeV kinetic energy transporting through a free space. The initial distribution of the beam is assumed to be semi-Gaussian, with transverse rms size of 0.5 mm, and transverse rms emittance of 0.5 μm. The initial longitudinal rms size is 1 mm and 0 rms longitudinal emittance. An electron inside the beam will be subject to Coulomb forces from other electrons. Here, we neglected scattering effects from other electrons and included only the mean field space-charge electromagnetic forces. The simulation was done using a quasi-static particle-in-cell code, IMPACT-T [11], to include the space-charge effects self-consistently. The electric and magnetic fields were computed by solving the three-dimensional Poisson equation in the beam frame and then transformed to the laboratory frame using the Lorentz transformation. The number of macroparticles used in this simulation is 1.28 millions with $64 \times 64 \times 64$ grid points. Fig. 7 shows transverse rms size evolution of the electron beam from the numerical simulation using the new integrator with 800 ps time step size and the Boris integrator with 800 ps step size together with a solution with much smaller 8 ps time step size. It is seen that the Boris integrator yields significantly larger rms size than the other two solutions. This suggests that given the same time step size, the new numerical integrator should be more accurate than the Boris integrator to simulate a relativistic electron beam including space-charge effects.

4. Conclusions and discussions

In this paper, we proposed a simple, fast second-order accuracy numerical integrator for relativistic charged particle tracking. It has less numerical error than the popular Boris integrator for tracking a relativistic electron subject to space-charge fields. It also requires less number of numerical operations than the relativistic Vay integrator. Recently, another time-reversible, volume preserving, second-order accuracy integrator was proposed to be valid for large relativistic factor [12] after the above work was done. This integrator replaces the γ_- in Eq. (17) by a new more complex γ, which is obtained from the solution of a quadratic equation. This integrator requires more numerical operations than the fast integrator proposed in this study.

The proposed second-order integrator for relativistic particle tracking has the advantages of simplicity and speed. Nevertheless, it is not time reversible, neither volume preserving. This may cause some numerical errors in long-term tracking. However, from above numerical

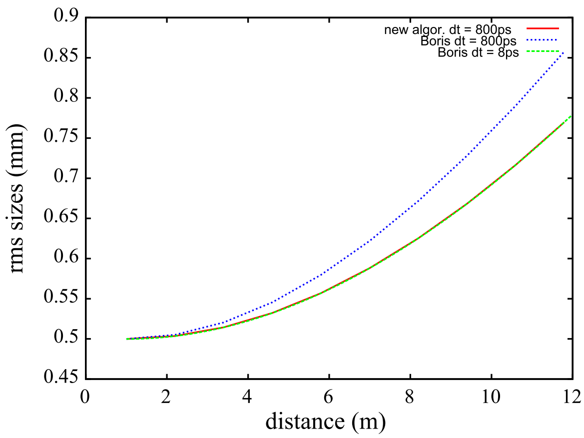

Fig. 7. Transverse rms size evolution of the electron beam from the new algorithm and the Boris algorithm with 800 ps time step size and the solution using much smaller 8 ps time step size.

example for tracking an electron through 500,000 periods, it appears that this integrator works quite well in preserving phase space structure along with the time-reversible Vay integrator.

Acknowledgements

Work supported by the U.S. Department of Energy under Contract No. DE-AC02-05CH11231. We would like to thank Dr. C. Mitchell for bringing author's attention to this study and useful discussions. This research used computer resources at the National Energy Research Scientific Computing Center.

References

[1] J. Boris, in: Proceedings of the Fourth Conference on the Numerical Simulation of Plasmas (Naval Research Laboratory, Washington, DC, 1970), pp. 3–67.
[2] H. Qin, S. Zhang, J. Xiao, J. Liu, Y. Sun, W.M. Tang, Phys. Plasmas 20 (2013) 084503.
[3] R. Zhang, J. Liu, H. Qin, Y. Wang, Y. He, Y. Sun, Phys. Plasmas 22 (2015) 044501.
[4] J.V. Vay, Phys. Plasmas 15 (2008) 056701.
[5] H.F. Baker, Proc. Lond. Math. Soc. 34 (1902) 347.
[6] J.E. Campbell, Proc. Lond. Math. Soc. 29 (1898) 14.
[7] F. Hausdorff, Math. Nat. 58 (1906) 19.
[8] C.K. Birdsall, A.B. Langdon, Plasma Physics via Computer Simulation, CRC Press, New York, 2004, p. 174 (p).
[9] A. Friedman, D.P. Grote, I. Haber, Phys. Fluids B 4 (1992) 2203.
[10] P. Stoltz, J. Cary, G. Penn, J. Wurtele, Phys. Rev. Spec. Top.-Accel. Beams 5 (9) (2002) 094001.
[11] J. Qiang, S. Lidia, R.D. Ryne, C. Limborg-Deprey, Phys. Rev. ST Accel. Beams 9 (2006) 044204.
[12] A.V. Higuera, J.R. Cary, Structure-preserving Second-order Integration of Relativistic Charged Particle Trajectories in Electromagnetic Fields. arXiv:05605v1, 2017.